RSC Advances

This is an *Accepted Manuscript*, which has been through the Royal Society of Chemistry peer review process and has been accepted for publication.

Accepted Manuscripts are published online shortly after acceptance, before technical editing, formatting and proof reading. Using this free service, authors can make their results available to the community, in citable form, before we publish the edited article. This *Accepted Manuscript* will be replaced by the edited, formatted and paginated article as soon as this is available.

You can find more information about *Accepted Manuscripts* in the Information for Authors.

Please note that technical editing may introduce minor changes to the text and/or graphics, which may alter content. The journal's standard Terms & Conditions and the Ethical guidelines still apply. In no event shall the Royal Society of Chemistry be held responsible for any errors or omissions in this *Accepted Manuscript* or any consequences arising from the use of any information it contains.

ROYAL SOCIETY OF CHEMISTRY

www.rsc.org/advances

Cite this: DOI: 10.1039/c0xx00000x

ARTICLE TYPE

www.rsc.org/xxxxxx

Pure-silica ZSM-22 Zeolite Rapidly Synthesized by Novel Ionic Liquid-directed Dry-gel-conversion

Haimeng Wen, Yu Zhou, Jingyan Xie, Zhouyang Long, Wei Zhang and Jun Wang*

Received (in XXX, XXX) Xth XXXXXXXXX 20XX, Accepted Xth XXXXXXXXX 20XX

DOI: 10.1039/b000000x

Shortening the crystallization process of zeolites is significant for their applications because of the energy saving. Here, we report a rapid synthetic route for pure-silica ZSM-22 zeolite with TON topology. The synthesis was achieved by dry-gel-conversion, where the dry gel was prepared under the unusual acidic condition for hydrolyzing the silica precursor with 1,3-alkylimidazolium ionic liquid as the structure directing agent (SDA). Highly crystallized pure-silica ZSM-22 can be synthesized within two days crystallization, dramatically shorter than ten percent of the conventional hydrothermal strategy. Using similar procedure, Al-containing ZSM-22 can also be synthesized by simply adding aluminum salt in the initial gel. In addition, understanding of the structure directing role of ionic liquids is attempted through characterizations of IR, TG, ^{1}H and ^{13}C NMR spectra.

Introduction

Zeolites are a vast class of crystalline porous materials that have been widely used as solid catalysts, ion exchangers, adsorbents and so on.[1] Zeolite synthesis usually goes through a hydrothermal treatment process with high temperatures, consuming large amounts energy. How to shorten the synthetic cycle, especially shorten the high-temperature hydrothermal process, is crucial for practical applications of zeolites, which strongly depends on developing new synthetic strategy. Many efforts have been made on aluminosilicate zeolites,[2] but rare attention is paid on pure-silica ones.

Pure-silica zeolites are of primary interest in both academic areas and practical applications due to their pure-silica framework, high hydrothermal stability, superior mechanical strength and hydrophobicity.[3] Besides, they are accessible in special applications, for example, in separating nonpolar from polar molecules owing to their electroneutral framework.[4] Up to now, besides the most widely studied silicalite-1,[5] only a few kind of zeolitic topologies can be achieved with a pure-silica framework, requiring deboronated borosilicate zeolite as seeding,[6] complex template[7] or additives like fluoride.[8] Among various zeolites, ZSM-22 is of TON topology with one-dimensional pore system (0.45 × 0.55 nm),[9] and has exhibited high catalytic activity and selectivity in paraffin isomerization,[10] butene isomerization,[11] aromatization reaction,[12] etc. Synthesis of the pure phase of ZSM-22 is still difficult, which usually employs dynamic hydrothermal method and needs the vertical speed higher than 400 rpm to avoid the formation of the often-combined impurity phases.[13] Meanwhile, Al-containing ZSM-22 can be synthesized in short time[14], but the synthesis of pure-silica ZSM-22 without impurity usually needs several weeks or even months for completed crystallization.[15]

Herein, we report a rapid synthesis of pure-silica ZSM-22 through dry-gel-conversion (DGC) method using ionic liquid (1-butyl-3-methylimidazolium bromide, [BMIm]Br) as the structure directing agent. Ionic liquids (ILs) are applied not only in chemistry but also in materials science due to their versatile properties.[16] When applied in zeolite synthesis, ionic liquids have been used as structure directing agent for the formation of MFI, BEA and ANA topologies,[17] and imidazolium-derived ionic liquids can be structurally manipulated to show good structure directing effect for pentasil zeolites.[18] A series of diquaternary organo-cations built upon N-methylimidazole have been used for synthesizing TON type zeolite with SiO_2/Al_2O_3 molar ratios 50~300,[19] and recently 1,3-alkylimidazolium-related ionic liquids have been attempted for synthesizing Al-containing TON topology which however was not successful for pure-silica one.[20]

The DGC method is an efficient route to synthesize zeolites because of its specific advantages. Unlike the conventional hydrothermal routes where the materials contact directly with water, DGC allows the solid gels contacting only with steam and inhibiting the potential of phase-separation.[21] The use of homogeneous gels benefits the formation of pure phase through preventing inhomogeneous crystallization that often occurs in the conventional static hydrothermal method.[22] Further, the high concentration of silica precursor in dry gel facilitates rapid nucleation and thus shortens the crystallization process. As far as we know, the ionic liquid-directed DGC route has not been reported before. In this work, the acid-hydrolysis route is used to prepare the dry gel.[23] Correspondingly, pure-silica ZSM-22 is rapidly synthesized with only two days crystallization. The other

RSC Advances Accepted Manuscript

1,3-alkylimidazolium-related ionic liquids with 2, 6, 8, 10, 12 and 14 carbons ([EMIm]Br, [HMIm]Br, [OMIm]Br, [DMIm]Br, [C_{12}MIm]Br and [C_{14}MIm]Br) are also investigated. Besides, Al-containing ZSM-22 is also synthesized by adding aluminum salt in the initial gel. Primary understanding of the structure directing effect is discussed through comparative experiments, as well as the IR, TG, ^{1}H and ^{13}C NMR analysis, though the exact crystallization mechanism of the present synthesis is unclear yet.

Experimental section

Synthesis

All chemicals in this study were analytical grade and used as received except the laboratory-made NaOH solution. A typical procedure for the pure-silica zeolite synthesis was carried out as follows. Firstly, the concentrated sulfuric acid (98 wt %) was slowly dripped into distilled water (1000 mL) to obtain an acidic solution (pH = 1.0). Then the acidic solution (25.20 g) and tetraethylorthosilicate (TEOS, 7.39 g) were mixed in a 100 mL glass beaker under vigorous stirring, and the obtained mixture was stirred at 298 K for 24 h for further hydrolysis of TEOS. To get a basic gel, [BMIm]Br was added into the above mixture, followed with the dropwise adding of NaOH solution (12.5 mol/L). The compositional molar ratio of the gel is 1 SiO_2: x [BMIm]Br : y Na_2O: 40 H_2O, in which x denotes the molar ratio of IL/SiO_2, and y denotes the molar ratio of Na_2O/SiO_2. Next, aging was conducted in a microwave reactor (CEM, Mars 240/50) at 333 K for 5 h. After aging, the gel was dried in oven at 373 K for 4 h and ground to powdered dry gel. Finally, the dry gel (0.5 g), which is amorphous as seen in the XRD pattern of Figure S1, was placed and sealed in a raised Teflon holder inside a 50 mL Teflon-lined steel autoclave involving distilled water (0.5 g) at the bottom for static crystallization at 443 K for 2 days under the autogenous pressure. After crystallization the resultant solid was filtered, washed with ethanol and distilled water, and dried at 373 K for 12 h to give the as-synthesized samples. The pure-silica ZSM-22 is obtained by calcining the as-synthesized sample at 823 K for 5 h in air stream to remove the ionic liquid. The obtained pure-silica ZSM-22 samples were named as ZX-Y, in which X = 100 × x, Y = 100 × y. Al-containing ZSM-22 (Al-ZSM-22) was synthesized similarly except that aluminum sulfate was added before adding [BMIm]Br, and the obtained samples were named as ZX-Y-Z, in which the second Z denotes the molar ratio of SiO_2/Al_2O_3 in the gel, X and Y are defined as before.

For comparison, we also prepared control samples to investigate the structure directing effect of ionic liquid. We synthesized samples following the above procedure in the absence of [BMIm]Br, which represents the SDA-free route. The structure directing agent 1,6-hexanediamine (HDA) for the conventional hydrothermal synthesis of ZSM-22 was also used for the present DGC method instead of [BMIm]Br. The gel was basic after adding 1,6-hexanediamine, so we added a small amount of dilute sulphuric acid instead of NaOH solution such that the gel pH value was the same as the case of [BMIm]Br. The ionic liquid SDA with 2, 6, 8, 10, 12 and 14 carbons in alkyl-tethered imidazolium were also investigated other than [BMIm]Br. The base-hydrolysis sample was prepared following the same procedure, except that the silicate precursor was prepared by catalytically hydrolyzing TEOS in NaOH medium (instead of acidic solution) at pH = 10. In addition to DGC, hydrothermal synthesis of ZSM-22 with [BMIm]Br as SDA was also tried, where the aged gel was directly transferred into a Teflon-lined stainless steel autoclave and crystallized statically at 443K for 2 days.

Characterization

The crystalline structure of the prepared samples were characterized by X-ray diffraction analysis (XRD) with a SmartLab diffractmeter from Rigaku equipped with a 9 kW rotating anode Cu source at 45 kV and 200 mA, from 5 ° to 50 ° with a scan rate of 0.2 °/s. The relative crystallinities of the ZX-Y series are calculated roughly from the variation of the peaks area in the XRD patterns, assuming crystallinity of 100% for the as-calcined Z35-19 sample. Morphologies of the samples were tested with a field-emission scanning electron microscope (SEM) instrument of Hitachi S-4800. The SiO_2/Al_2O_3 molar ratio of the final solid was measured using ADVANT'XP X-ray fluorescence spectrometer (Thermofisher Scientific). Specific surface area and pore volume of the calcined sample was obtained from N_2-adsorption-desorption isotherms using multipoint BET and t-plot methods. The samples were outgassed at 573 K for 3 h prior to the measurements. Isotherms were obtained at liquid nitrogen temperature with a BEL SORP-MAX analyzer. FT-IR spectra were recorded on a Nicolet iS10 FT-IR instrument (KBr disks) in the 4,000~500 cm^{-1} region. The morphology and microstructure of pure-silica ZSM-22 was determined by transmission electron microscopy (TEM) using a JEM-2100 F. Thermogravimetric (TG) analysis was carried out with a STA 409 instrument in dry air at a heating rate of 10 ^{o}C min^{-1}. ^{29}Si MAS NMR spectrum was recorded on a Bruker Avance 400D multinuclear solid-state magnetic resonance spectrometer. Solid state ^{13}C and ^{1}H spin-echo pulse NMR spectra were recorded with a magnetic field of 9.4 T.

Results and discussion

DGC synthesis of pure-silica ZSM-22

Figure 1A shows the XRD patterns of as-synthesized samples ZX-Y series obtained with dry gels containing different amounts of [BMIm]Br and Na_2O. All the samples give the high-resolution peaks characterized for the TON-topologized zeolite without any peaks attributable to cristobalite or ZSM-5 that usually jointly occur in static hydrothermal synthesis of ZSM-22.[13] After calcination for removal of the SDA, the XRD patterns of all the samples exhibit similar peaks to as-synthesized ones with enhanced intensities of some lines, especially the peak assigned to the 110 crystal plane (Figure 1B), implying the increase of the crystallinity and long range order of the structure as a consequence of the reduction of the electron density in the channel due to the elimination of molecules trapped within the channels.[24] Moreover, no additional peak assigned to other zeolite phase is detected in the XRD patterns of the calcined samples, suggesting that the DGC method using IL as SDA is comfortable for the rapid synthesis of pure-silica ZSM-22.

In the synthesis, it can be found that the concentrations of [BMIm]Br and Na_2O exert significant influences on the crystallinity of pure-silica ZSM-22. In the case of the low

RSC Advances Accepted Manuscript

This journal is © The Royal Society of Chemistry [year]

concentration of [BMIm]Br and Na_2O (x = 0.15 and y = 0.15), the relative crystallinity of obtained sample Z15-15 is 33% (curve a, Figure 1B). Keeping the IL concentration constant and increasing the Na_2O amount to y = 0.19, the obtained Z15-19 sample presents enhanced diffraction intensities (curve b, Figure 1B), showing a relative crystallinity of 57%. The impurity phase of magadiite emerges when increasing the Na_2O amount to y = 0.22 (curve a, Figure S2) and becomes dominating at higher Na_2O concentration of y = 0.24 (curve b, Figure S2), indicating that a moderate Na_2O amount favors high crystallinity. Fixing the Na_2O amount of y = 0.19 while raising the IL amount up to x = 0.35, the relative crystallinities of obtained ZX-19 series are increased from 57% to 100% (curve b-d, Figure 1B), suggesting that a higher concentration of IL favors better crystallinity. Further increasing the IL to x = 0.45, the synthesized Z45-19 shows a relative crystallinity of 72% (curve e, Figure 1B). It has been revealed that the amount of structure directing agent is closely related to the colloidal properties which influences zeolitic crystal growth in the followed crystallization process.[25] It is suggested in this work that the large amount of IL in initial gel is not beneficial to the drying process while the water in the undried gel is disadvantageous for the DGC process.[26] Therefore, suitable concentration of the IL is important for the fabrication of highly crystallized pure-silica ZSM-22.

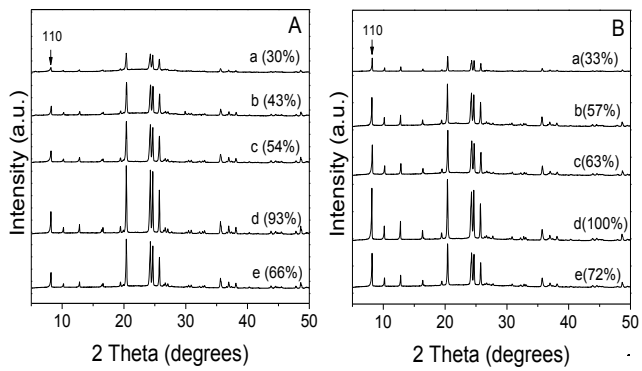

Figure 1. XRD patterns of (A) as-synthesized pure-silica ZSM-22 and (B) as-calcined pure-silica ZSM-22: (a) Z15-15, (b) Z15-19, (c) Z25-19, (d) Z35-19 and (e) Z45-19.

The synthesis of the pure phase of highly crystallized silica-ZSM-22 is a complicated process affected by various parameters. Positive structure directing effect of imidazole-based ILs for synthesizing pentasil zeolite has been mentioned previously.[18] In our synthesis route, the effect of IL [BMIm]Br is investigated by manipulating a SDA-free synthesis procedure. The XRD pattern (curve a, Figure 2A) shows that the sample synthesized in the absence of [BMIm]Br exhibits the phase of magadiite rather than ZSM-22, suggesting that [BMIm]Br should have acted as SDA for the formation of TON structure. Synthesis of pure-silica ZSM-22 with other SDA was also conducted. Considering that the traditional SDAs in hydrothermal synthesis of ZSM-22 are linear amine salts, polyamine and vinyl-pyridine,[27] we choose the commonly used 1,6-hexanediamine (HDA) as the structure directing agent instead of [BMIm]Br in the present DGC route. Following the same procedure, only amorphous phase forms (curve b, Figure 2A), indicating that [BMIm]Br plays an irreplaceable structure directing role. Actually, only one report has appeared for the vapor phase transport synthesis of Al-ZSM-22, in which the mixed vapor phase of diethylamide (Et_2N) and water was employed.[28] The resulting materials were mostly either cristobalite or quartz together with ZSM-22 zeolite, and the crystallization of pure phase ZSM-22 needed 7-12 days long-time at 443 K. On the contrary, the present [BMIm]Br IL-directed DGC synthesis favours the nucleation of ZSM-22 zeolite and promotes the rapid crystallization.

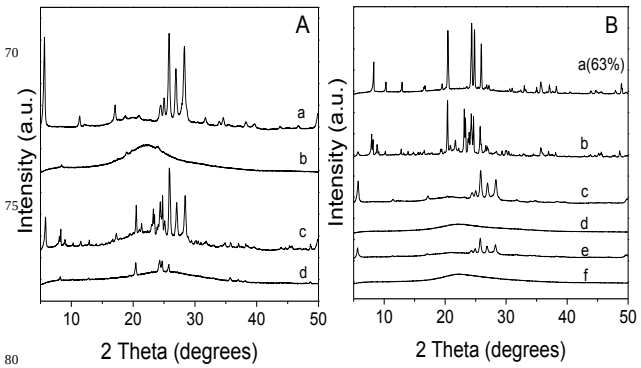

Figure 2. XRD patterns of (A) control samples obtained by (a) SDA-free route with the composition of 1 SiO_2: 0.19 Na_2O : 40 H_2O; (b) using 1,6-hexanediamine (HDA) as SDA with composition of 1 SiO_2: 0.25 HDA : 40 H_2O; (c) hydrothermal synthesis after microwave aging step and crystallized at 443 K for 2 days, (d) base-hydrolysis of TEOS and DGC method with the gel composition of 1 SiO_2: 0.35 [BMIm]Br : 0.19 Na_2O: 40 H_2O and crystallization at 443 K for 2 days; (B) samples obtained using (a) [EMIm]Br, (b) [HMIm]Br, (c) [OMIm]Br, (d) [DMIm]Br, (e) [C_{12}MIm]Br and (f) [C_{14}MIm]Br as SDA with the composition of 1SiO_2: 0.35 IL: 0.19 Na_2O: 40 H_2O.

For comparison, hydrothermal synthesis of pure-silica ZSM-22 was conducted at 443 K for 2 days after microwave aging of the gel with the same composition as Z35-19. The XRD pattern of thus obtained material demonstrates weak peaks of ZSM-22 mixed with magadiite (curve c, Figure 2A), suggesting that the DGC method also contributes the rapid formation of the pure phase of all-silica TON structure. Taking together the fact that the ionic liquid-free dry gel conversion cannot form pure-silica ZSM-22 (curve a, Figure 2A), it is drawn that both ionic liquid and dry-gel conversion procedure are indispensible for successful rapid synthesis of pure-silica ZSM-22.

The nature of silica precursors plays an important role in the formation of final zeolite phase. Dissolution of silica precursors is more important, through which silicate intermediates are formed followed by the onset of nucleation and crystallization.[29] When TEOS is hydrolyzed in basic rather than acidic condition, the obtained pure-silica ZSM-22 sample only presents very weak diffraction intensities (curve d, Figure 2A), reflecting a low crystallinity. In fact, TEOS can be catalytically hydrolyzed at acidic or basic conditions, causing different nucleation and growth rate of the silica precursors. In the acid-catalyzed system, the polymerization rate is more rapid than the hydrolysis rate. After the hydrolytic polymerization, a continuous linear three-dimensional cross-linked network forms, leading to small cage-like units. In contrast, the basic hydrolysis system causes a slower

RSC Advances Accepted Manuscript

polymerization rate than hydrolysis, which gives rise to short-chain cross-linked larger precursor particles. The resultant different primary structures are largely relative to nucleation rates in these systems.[30] Therefore, the acidic condition for preparing silica precursor is crucial for the present DGC method.

To study the influence of the alkyl chain length on the structure directing effect of alkylimidazolium IL, alkyl chains with 2, 6, 8, 10, 12 and 14 carbon atoms were tethered onto imidazolium ring for DGC synthesis of ZSM-22 instead of the lead SDA ([BMIm]Br). Figure 2B shows the XRD patterns of the pure-silica ZSM-22 samples using that series of IL SDAs. When using 1-ethyl-3-methylimidazolium bromide as the SDA, the obtained sample still gives diffraction peaks attributing to the pure phase TON structure (curve a, Figure 2B), similar to Z35-19 directed by [BMIm]Br but with the relative crystallinities of 63%. In the case of longer alkyl chains, 1-hexyl-3-methylimidazolium bromide produces a mixture of TON and MFI type frameworks (curve b, Figure 2B), and the further increase of the carbon chains up to 8, 10, 12 and 14 causes no ZSM-22 structure but magadiite or amorphous phases (curves c-f, Figure 2B). Therefore, the successful synthesis of pure-silica ZSM-22 by DGC route depends partially on the alkyl chain length of alkylimidazolium IL. Moreover, the calculated channel size along the ten-member ring pores in per unit cell of ZSM-22 is about 1.08 ± 0.04 nm.[27] The molecular size of [BMIm]Br is about 1 nm along the alkyl chain direction[18,31], well matching the channel size of ZSM-22. Contrastively, the length of 1-hexyl-3-methylimidazolium (ca. 1.308 nm based on per C-C length 0.154 nm) is larger than the channel size of ZSM-22, let alone the other longer alkylimidazoliums with alkyl carbon chains of 8, 10, 12 and 14, accounting for the unsuccessful synthesis of pure phase silica-ZSM-22. It is 1-butyl-3-methylimidazolium bromide that to be the most effective SDA in the ionic liquid-directed DGC synthesis of TON zeolites.

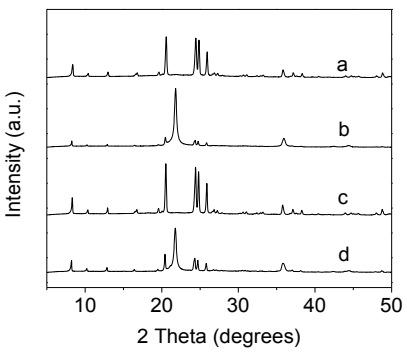

Figure 3. XRD patterns for as-synthesized (a, c) and as-calcined samples (b, d), obtained through heating aging at 60 °C, 5 h (a, b) and 25 °C, 24 h (c, b).

The influence of microwave aging process is investigated by the control experiment with the traditional heating aging. As shown in Figure 3, the as-synthesized pure-silica ZSM-22 can be obtained with heating aging by adjusting aging temperature and time, but crystallinities are low. Moreover, the intensity of XRD peaks decreased and quartz phase occurred after calcination, suggesting that the heating aging is not suitable to obtain stable ZSM-22. Therefore, the microwave aging plays an important role in our rapid synthetic route, mostly due to the promoted nucleation and growth of preliminary zeolitic units. Influences of water content in the dry gel and crystallization temperature are also studied, where it is interesting to observe that another pure-silica zeolite ZSM-48 can be synthesized through the present IL-directed DGC method by adjusting the water content in dry gel and the temperature for crystallization (Figure S3), though crystallinity is not high as yet. Such phenomenon suggests the possibility that some other zeolite phases can be also achieved using our method.

Textural properties of synthesized pure-silica ZSM-22

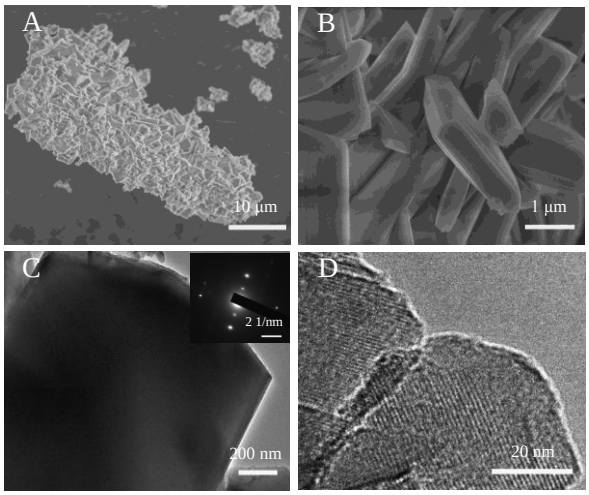

Figure 4. (A, B) SEM and (C, D) TEM images of as-calcined Z35-19 sample. The inset part of TEM image is the simultaneously recorded SAED pattern from the particle.

Figure 4A and 4B shows the SEM images of the selected pure-silica ZSM-22 sample Z35-19, exhibiting the morphology of aggregation of irregular micron size prism stacked by thin sheets. The traditional morphology of hydrothermally synthesized ZSM-22 is needle-like crystals with a smaller size. Alfaro et al.[32] have obtained a similar conclusion by comparing the DGC synthesized silicalite-1 zeolite and that through hydrothermal synthesis. The concentration of raw materials in a hydrothermal system is low because of the large amount of water. The low concentration inhibits the adjacent and aggregation of nuclei during crystal growth, usually causing small crystals. In DGC, a large number of nuclei aggregate because of the limited amount of water, which results in the aggregated morphology with significantly larger sizes. Figure 4C and 4D describes the TEM images and selected area electron diffraction pattern for Z35-19. A clear and well defined prism plus the ordered microporous channels can be observed, with the selected area electron diffraction further proving the crystal structure.

Figure 5A shows nitrogen adsorption-desorption isotherm for the as-calcined Z35-19 sample. The isotherm is type I, according with the typical microporous structure. There is a high nitrogen uptake at low relative pressures ($P/P_0 < 0.1$), with the BET surface area of 248 $m^2\ g^{-1}$ and pore volume of 0.14 $cm^3\ g^{-1}$. The

RSC Advances Accepted Manuscript

This journal is © The Royal Society of Chemistry [year]

as-calcined Z35-19 is further studied by ^{29}Si NMR spectroscopy. As shown in Figure 5B, there are strong signals at ca. -110, -112 and -113 ppm, indicating that most of the silicon atoms are in four-connected sites (Q^4) as expected for a framework silicate. The only weak peak at ca. -100 ppm suggests the presence of Q^3 sites in a small amount, indicative of structural defects. The above characterizations present a well zeolitic structure for Z35-19, validating that our DGC method is able to prepare highly crystallized pure-silica ZSM-22.

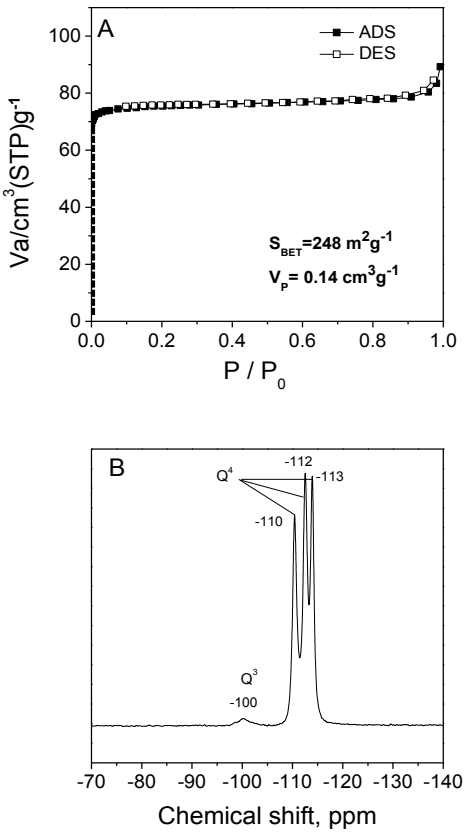

Figure 5. (A) N_2 adsorption-desorption isotherm and (B) ^{29}Si MAS NMR spectrum of as-calcined Z35-19 sample.

DGC synthesis of Al-ZSM-22

The ZSM-22 zeolite synthesized above is in pure-silica state. Indeed, it is much valuable to try Al-containing gels for the succeeding DGC process. Figure 6 shows the XRD patterns of the as-synthesized and as-calcined Al-containing ZSM-22 samples with the SiO_2/Al_2O_3 molar ratios of 200, 150, 100 and 50. As the aluminum amount is raised, the peak intensity decreases, reflecting the decline of crystallinity. When SiO_2/Al_2O_3 reduces to 50, there is no zeolite phase observed (curve d, Figure 6A). After calcination, the samples with SiO_2/Al_2O_3 of 200 and 150 present similar XRD patterns as the as-synthesized parents but with strengthened peak intensities, while the sample with SiO_2/Al_2O_3 of 100 displays an additional peak at 21.7 °, indicating the occurrence of an impurity phase upon calcination. The SiO_2/Al_2O_3 molar ratios of the final zeolite products Al-ZSM-22 were measured by XRF analysis and summarized in Table 1. The results indicated that the SiO_2/Al_2O_3 ratios of the obtained Al-ZSM-22 are slightly lower than those of their parent gels. The adding of aluminum in the synthesis will cause a complex interaction among silica precursor, aluminum source, Na^+ cation and ionic liquid. Zones[18] has reported an inhibitory effect of aluminum amount on zeolite crystallization referring to the synthesis of pentasil zeolites in the presence of quaternary imidazole compounds. In order to obtain the highly crystallized Al-ZSM-22 in a wide range of SiO_2/Al_2O_3 ratio, further adjusting of the dry gel composition and crystallization condition may be essential.

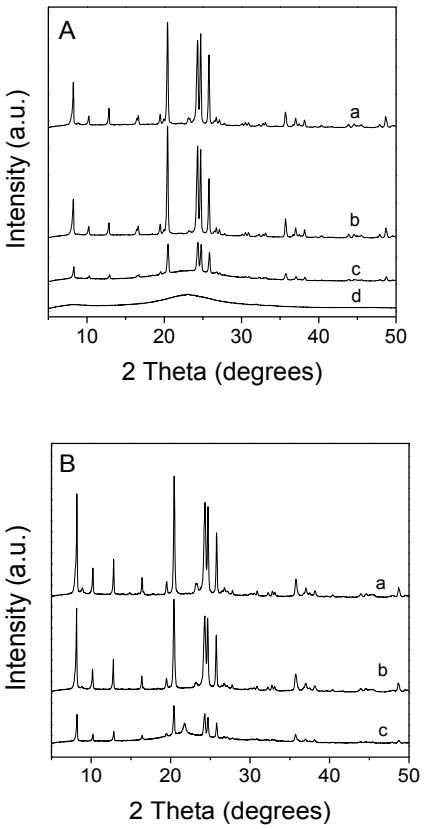

Figure 6. XRD patterns of (A) as-synthesized and (B) as-calcined Al-ZSM-22: (a) Z35-19-200, (b) Z35-19-150, (c) Z35-19-100 and (d) Z35-19-50.

Table 1 SiO_2/Al_2O_3 molar ratios of the synthesized Al-ZSM-22 samples

Sample	SiO_2/Al_2O_3 (mol/mol)	
	Gel mixture	As-calcined Al-ZSM-22
Z35-19-200	200	152
Z35-19-150	150	123
Z35-19-100	100	93

RSC Advances Accepted Manuscript

Preliminary understanding of structure directing effect of ionic liquid

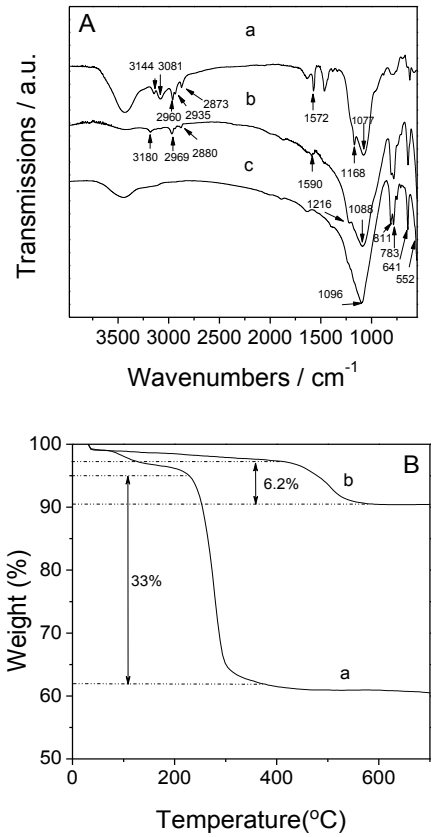

Figure 7. (A) FT-IR spectra of (a) dry gel, (b) as-synthesized and (c) as-calcined Z35-19; (B) TG curves of (a) dry gel and (b) as-synthesized Z35-19.

FT-IR, TG, ^{1}H and ^{13}C NMR spectra are used to characterize the dry gel and the resulting pure-silica ZSM-22 sample Z35-19, aiming to further understand the structure directing role of [BMIm]Br in the DGC process. Figure 7A shows the FT-IR spectra of the dry gel, as-synthesized and as-calcined Z35-19 sample. The dry gel shows vibrations for the BMIm cation in ranges of 1100-1600 and 2700-3200 cm^{-1} (curve a, Figure 7A). The bands at 1572 and 1168 cm^{-1} are attributed to the imidazole C=N and C-N stretching vibrations. The C-H bands for imidazolium ring appear at 3144 and 3081 cm^{-1}. Moreover, the bands at 2960, 2935 and 2878 cm^{-1} are attributed to aliphatic C-H bending vibrations.[33] The above result indicates that the ionic liquid is well preserved in dry gel, i.e., it has not been decomposed throughout the acid-hydrolysis, the subsequent alkaline aging, and the final drying processes. Even when the crystallization is completed, partial bands mentioned above can be observed though the intensity is weak, which is attributed to the existing of ionic liquid in the as-synthesized ZSM-22 (curve b, Figure 7A). All the peaks for BMIm cation disappear after calcination and the peak intensities of TON framework become stronger at 552, 641, 783, 811 and 1096 cm^{-1} (curve c, Figure 7A), reflecting the removal of the SDA with well retaining of the zeolite framework. Figure 7B displays the TG curves of the dry gel and as-synthesized product of Z35-19. The small weight loss below 200 °C is attributed to physically adsorbed water in both two samples. At higher temperatures, the dry gel presents a large weight loss of about 33% ranging from 220 to 370 °C, attributable to the decomposition of [BMIm]Br. The decomposition temperature of the gel-involved [BMIm]Br is similar to the free IL, reflecting a weak interaction between the SDA and the silica precursor. On the contrary, the as-synthesized Z35-19 displays a slower weight loss till 420 °C, and the weight loss in the range 200~420 °C is related to the removal of water in zeolitic internal pores. A dramatic weight loss of 6.2% is observed over 420 °C due to the decomposition of [BMIm]Br. The weight loss 6.2% is much lower than that for the dry gel. Such phenomena indicate that the SDA amount in the final zeolite is much lower than that in the dry gel. This is why the as-synthesized Z35-19 sample presents weak peaks in the IR spectrum. Calculated from the weight loss (6.2%) and the molecular weight of [BMIm]Br (219.12 g mol^{-1}), there is about 1.7×10^{20} [BMIm]Br molecules per gram zeolite Z35-19. Owing to the space confine, the [BMIm]Br molecules are located in the zeolite channel by adopting end by end mode. Therefore, the occupied space of one [BMIm]Br molecule in Z35-19 channel is about 8.2×10^{-22} cm^3. Correspondingly, the total occupied space of all the [BMIm]Br molecules in Z35-19 channel is about 0.138 cm^3 g^{-1}, in according with the pore volume of Z35-19 (0.14 cm^3 g^{-1}), suggesting the complete filling of the zeolite pores with [BMIm]Br (Figure 8b and 8c) just as the role 1,6-hexanediamine played in hydrothermal synthesis of ZSM-22.[27] Such phenomenon further interprets why the [BMIm]Br exerts well

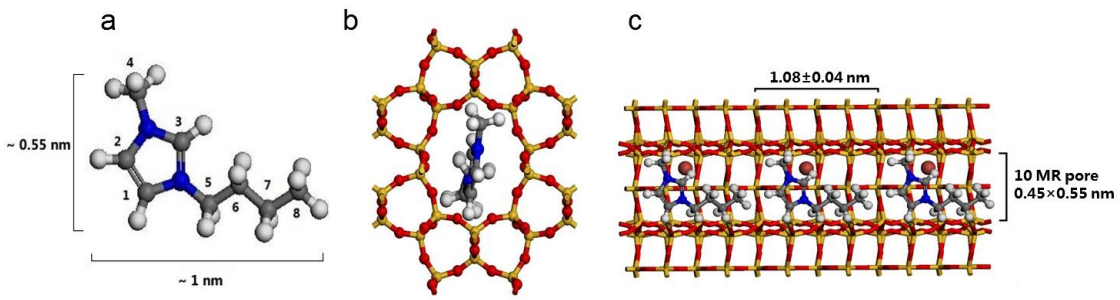

Figure 8. a) Ball and stick model of 1-butyl-3-methylimidazolium cation template; the illustration of the potential state of the ionic liquid template in the microporous channel of TON type framework viewing b) along the pore axis and (c) perpendicular to the pore axis

This journal is © The Royal Society of Chemistry [year]

RSC Advances Accepted Manuscript

structure directing effect for the synthesis of TON zeolite. Moreover, the decomposition temperature of the IL is much higher for the as-synthesized sample than the gel, mainly because the IL SDA has been encapsulated in the channels of the zeolite (schematically illustrated in Figure 8c).This result provides an important clue for understanding the IL structure directing effect for the DGC synthesis of pure-silica ZSM-22.

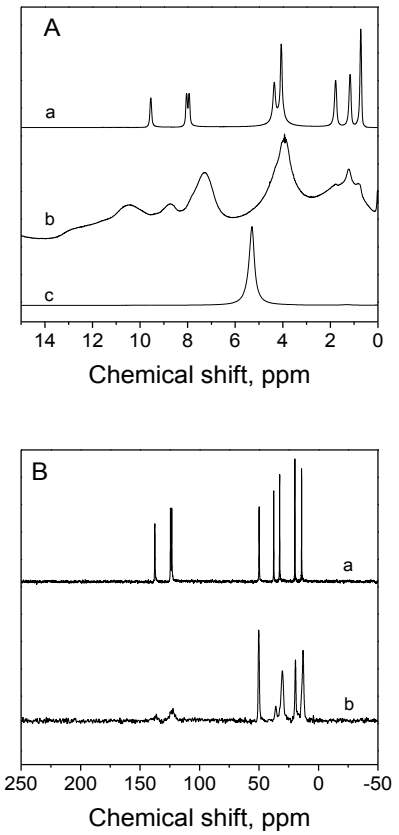

Figure 9. (A) ^{1}H NMR spectra of (a) dry gel, (b) as-synthesized and (c) as-calcined Z35-19; (B) ^{13}C MAS NMR spectra of (a) dry gel and (b) as-synthesized Z35-19.

Figure 9A shows the ^{1}H NMR spectra of the dry gel, as-synthesized and as-calcined Z35-19 sample. The dry gel shows eight peaks at 0.74, 1.18, 1.80, 4.05, 4.36, 7.92, 8.03 and 9.58 ppm (curve a, Figure 9A), similar to the signals of pure [BMIm]Br,[34] further indicating that the IL is preserved in the gel and exists as the free state. Differently, only broad and weak signals appear for the as-synthesized pure-silica ZSM-22 (curve b, Figure 9A) because of the low SDA amount. In addition, a shift of the signals for the H atoms of the imidazolium rings is observed, suggesting a strong interaction between IL and zeolite framework, as reflected by the IR and TG results above. The H-signals attributed to IL disappear after calcination, instead a signal at ca. 5 ppm is observed (curve c, Figure 9A) as a result of the presence of water in as-calcined pure-silica ZSM-22. The ^{13}C chemical shifts for the dry gel and as-synthesized Z35-19 are shown in Figure 9B. Peaks attributed to the C atoms belonging to imidazolium ring and aliphatic chain can be clearly seen in dry gel in the ranges of 100-150 and 0-50 ppm[17], respectively (curve a, Figure 9B). Signals at 14.38, 20.02, 32.56, 37.83, 50.04, 123.28, 124.39 and 137.64 ppm are attributed to the eight carbons of [BMIm]Br (Figure 8a). After crystallization in DGC synthesis, all these signals are still observed but with slightly shifts and declined intensities (curve b, Figure 9B) due to the lower IL content and the strong interaction between IL and zeolite framework, in good accordance with the results of IR, TG and ^{1}H NMR spectra.

The above analysis demonstrates that the IL [BMIm]Br first exists in the dry gel, and then interacts with the silica precursor and locates in the microporous channel to cause the formation of TON framework through a structure directing effect in our DGC synthetic route.

Conclusions

A rapid dry-gel-conversion synthetic route is developed to synthesize pure-silica ZSM-22 zeolite with acid-catalyzed hydrolysis of TEOS for preparing the dry gel and using ionic liquid [BMIm]Br as the structure directing agent. The ionic liquid plays the structure directing role in the synthesis and the dry-gel-conversion method contributes to the fast crystallization. The crystallization process is much shorter than conventional hydrothermal process, therefore promoting the potential to prepare functional pure silica TON topology zeolites such as zeolite membrane or aluminium free heteroatom zeolites.

Acknowledgements

The authors thank the National Natural Science Foundation of China (Nos. 21136005, 21303038 and 21476109), Jiangsu Province Science Foundation for Youths (No. BK20130921) and Specialized Research Fund for the Doctoral Program of Higher Education (No. 20133221120002).

Notes and references

State Key Laboratory of Materials-Oriented Chemical Engineering, Nanjing Tech University, Nanjing 210009, China
Fax: (+ 86)-25-83172261, Tel: (+86)-25-83172264, E-mail: junwang@njtech.edu.cn.

† Electronic Supplementary Information (ESI) available:[Additional XRD patterns and SEM image of samples]. See DOI: 10.1039/b000000x/

1 A. Corma, Chem. Rev. 1997, **97**, 2373; M.E. Davis, Nature 2002, **417**, 813; Y. Tao, H. Kanoh, L. Abrams and K. Kaneko, Chem. Rev. 2006, **106**, 896.
2 S. Inagaki, Y. Tsuboi, Y. Nishita, T. Syahylah, T. Wakihara and Y. Kubota, Chem. Eur. J. 2013,**19**, 7780; N. Sapawe, A.A. Jalil, S. Triwahyono, M.I.A. Shah, R. Jusoh, N.F.M. Salleh, B.H. Hameed and A.H. Karim, Chem. Eng. J. 2013, **229**, 388.
3 D.S. Wragg, R. Morris, A.W. Burton, S.I. Zones, K. Ong and G. Lee, Chem. Mater. 2007, **19**, 3924.
4 J. Stelzer, M. Paulus, M. Hunger and J.Weitkamp, Micropor. Mesopor. Mater. 1998, **22**, 1.
5 E.M. Flanigen, J.M. Bennett, R.W. Grose, J.P. Cohen, R.L. Patton and R.M. Kirchner, Nature 1978, **271**, 512.
6 J.C. Waal, M.S. Rigutto and H. Bekkum, J. Chem. Soc. Chem. Commun. 1994, 1241.
7 A. Corma, F. Rey, J. Rius, M.J. Sabater and S. Valencia, Nature 2004, **431**, 287.
8 X. Yang, M.A. Camblor, Y. Lee, H. Liu and D.H. Olson, J. Am. Chem. Soc. 2004, **126**, 10403.

RSC Advances Accepted Manuscript

9 G.T. Kokotailo, J.L. Schlenker, F.G. Dwyer and E.W. Valyocsik, Zeolites 1985, **5**, 349.

10 G. Wang , G. Liu, W. Su, X. Li, Z. Jiang, X. Fang, C. Han and C. Li, Appl. Catal. A, 2008, **335**, 20; J.F. Denayer, G.V. Baron, G. Vanbutsele, P.A. Jacobs and J.A. Martens, Chem. Eng. Sci. 1999, **54**, 3553.

11 R. Byggningsbacka, L.E. Lindfors and N. Kumar, Ind. Eng. Chem. Res. 1997, **36**, 2990; J.I. Villegas, M. Kangas, R. Byggningsbacka, N. Kumar, T. Salmi and D.Y. Murzin, Catal. Today. 2008, **133-135**, 762.

12 N. Kumar, L.E. Lindfors and R. Byggningsbacka, Appl. Catal. A 1996, **139**, 189.

13 M.A. Asensi, A. Corma, A. Mart ńez, M. Derewinski, J. Krysciak and S.S. Tamhankar, Appl. Catal. A: Gen. 1998, **174**, 163; D. Masih, T. Kobayashi and T. Baba, Chem. Commun. 2007, 3303.

14 E.W. Valyocsik, US Patent, 4902406.

15 B. Marler, Zeolites 1987, **7**, 393; J.J. Williams, Z.A.D. Lethbridge, G.J. Clarkson, S.E. Ashbrook, K.E. Evans and R.I. Walton, Micropor. Mesopor. Mater. 2009, **119**, 259.

16 T. Welton, Chem. Rev. 1999, **99**, 2071; K.R. Seddon, Nat. Mater. 2003, **2**, 363.

17 R. Kore, R. Srivastava, Catal. Commun. 2012, **18**, 11; R. Kore, B. Satpati and R. Srivastava, Chem. Eur. J. 2011, **17**, 14360; J.M.M. Blanes, B.M. Szyja, F. Romero-Sarria, M.Á. Centeno, E.J.M. Hensen, J. A. Odriozola and S. Ivanova, Chem. Eur. J. 2013, **19**, 2122; R. Kore, R. Srivastava, RSC Adv. 2012, **2**, 10072.

18 S.I. Zones, Zeolites, 1989, **9**, 458.

19 S.I. Zones, A.W. Burton, J. Mater. Chem. 2005, **15**, 4215.

20 Y. Tian, M.J. Mcpherson, P.S. Wheatley and R.E. Morris, Z. Anorg. Allg. Chem. 2014, **640(6)**, 1177.

21 S. S.A. Zaidi, S. Rohani, Rev. Chem. Eng. 2005, **21(5)**, 265.

22 J. Zhou, Z. Hua, J. Zhao, Z. Gao, S. Zeng and J. Shi, J. Mater. Chem. 2010, **20**, 6764.

23 Y. Wu, J. Wang, P. Liu, W. Zhang, J. Gu and X. Wang, J. Am. Chem. Soc. 2010, **132**, 17989; J. Gu, Y. Jin, Y. Zhou, M. Zhang, Y. Wu and J. Wang, J. Mater. Chem. A, 2013, **1**, 2453; F. Cao, Y. Wu, J. Gu and J. Wang, Mater. Chem. Phys. 2011, **130**, 727; J. Wang, J. Xie, Y. Zhou and J. Wang, Micropor. Mesopor. Mater. 2013, **171**, 87.

24 M. Milanesio, G. Artioli, A.F. Gualtieri, L. Palin and C. Lamberti, J. Am. Chem. Soc. 2003, **125**, 14549.

25 O. A. Fouad, R. M. Mohamed, M. S. Hassan and I. A. Ibrahim, Catal. Today, 2006, **116**, 82.

26 S. P. Naik, A.S.T. Chiang and R.W. Thompson, J. Phys. Chem. B 2003, **107**, 7006.

27 S. Ernst, Appl. Catal. 1989, **48**, 137.

28 S.G. Thoma, D.E. Trudell, F. Bonhomme and T.M. Nenoff, Micropor. Mesopor. Mater. 2001, **50**, 33.

29 S. Mintova, V. Voltchev, Micropor. Mesopor. Mater. 2002, **55**,171.

30 J. Šefčík, A.V. McCormick, Catal. Today, 1997, **35**, 205; B. Tan, S. E. Rankin, J. Phys. Chem. B, 2006, **110**, 22353.

31 L. Wang, L. Chang, L. Wei, S. Xu, M. Zeng and S. Pan, J. Mater. Chem, 2011, **21**,15732.

32 S. Alfaro, M.A. Valenzuela and P. Bosch, J. Porous Mater. 2009, **16**, 337.

33 G.R. Rao, T. Rajkumar and B. Varghese, Solid. State. Sci. 2009, **11**, 36; Y. Leng, J. Liu, P. Jiang and J. Wang, Catal. Commun. 2013, **40**, 84.

34 P. Zhao, M. Zhang, Y. Wu and J. Wang, Ind. Eng. Chem. Res. 2012, **51**, 6641.

RSC Advances Accepted Manuscript

This journal is © The Royal Society of Chemistry [year]

Table of contents

Pure-silica ZSM-22 Zeolite Rapidly Synthesized by Novel Ionic Liquid-directed Dry-gel-conversion

Haimeng Wen, Yu Zhou, Jingyan Xie, Zhouyang Long, Wei Zhang, and Jun Wang*

State Key Laboratory of Materials-Oriented Chemical Engineering, College of Chemistry and Chemical Engineering, Nanjing Tech University, Nanjing 210009, China.

* Corresponding author, e-mail: junwang@njtech.edu.cn

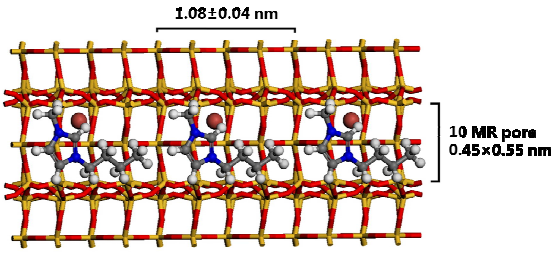

Rapid synthesis of pure-silica ZSM-22 was achieved through dry-gel-conversion process by using ionic liquid as the structure directing agent.

RSC Advances Accepted Manuscript